J Surfact Deterg (2019) **22:** 731–742
DOI 10.1002/jsde.12281

ORIGINAL ARTICLE

Solution Properties of Alkyl β-D-Maltosides

Zhencao Li[1] · Guoyong Chen[1] · Langqiu Chen[1] · Yanhua Zhang[1] · Zhiyong Dai[2]

Received: 7 December 2017 / Revised: 6 October 2018 / Accepted: 26 February 2019

Abstract Alkyl β-D-maltosides are an important class of sugar-based nonionic surfactants and have been widely studied. Nevertheless, it is still necessary to investigate further their amphiphilic structure-surface property relationships. In this article, we reported a series of properties of synthetic alkyl β-D-maltosides (**6a**–**6i**, n = 6–18) including their hydrophilic–lipophilic balance (HLB) number, water solubility, hygroscopicity, moisture-retention capacity, foaming ability, surface tension, thermotropic phase behavior, and skin irritation. Their HLB number and water solubility decreased with increasing alkyl chain length. Hexyl β-D-maltoside exhibited the strongest hygroscopicity and moisture-retention capacity. Decyl β-D-maltoside and dodecyl β-D-maltoside possessed excellent foaming power and foaming stability. Furthermore, the critical micelle concentration (CMC) of alkyl *β-D*-maltoside (**6a**–**6g**, n = 6–14) and their surface tension at CMC decreased with increasing alkyl chain length. At last, alkyl β-D-maltosides (**6a**–**6g**) should be considered as safe surfactants by the skin irritation assessment.

Supporting information Additional supporting information may be found online in the Supporting Information section at the end of the article.

✉ Langqiu chen
chengood2003@263.net

[1] College of Chemistry, Key Laboratory of Environmentally Friendly Chemistry and Application of Ministry of Education, Xiangtan University, Xiangtan, 411105, Hunan, People's Republic of China Republic of China

[2] Ausnutria Dairy (China) Co. Ltd., Changsha, 410005, Hunan, People's Republic of China

Keywords Nonionic surfactants · Surface activity · Foaming property · Interfacial science

J Surfact Deterg (2019) **22:** 731–742.

Introduction

Alkyl polyglycosides (APG) are a class of nonionic surfactants, they are derived from sugars and fatty alcohols (Abel et al., 2011; Aripin et al., 2012; Zhao et al., 2017). Apart from an excellent performance in terms of surface tension, foamability, and detergency, APG are environmentally friendly, biodegradable, and low-toxic surfactants. Thereby, they can be used for various applications such as drug carriers, intranasal adjuvants, silk degumming agents, and in oil recovery and sludge anaerobic fermentation (Ahmad et al., 2014; Faramarzi et al., 2017; Karam et al., 2017; Wang and Zhang, 2017; Wu et al., 2017; Xiao et al., 2017; Zhou et al., 2017).

Alkyl D-maltosides could be prepared using a glycochemistry method from the renewable raw materials, D-maltose and aliphatic alcohols. They could be categorized as ecologically safe sugar-based surfactants (Ahmad et al., 2014; Aripin et al., 2012; Karam et al., 2017; Zhao et al., 2017). From a chemical point of view, alkyl D-maltosides are stable under neutral and alkaline conditions because they are comprised of bulkier and rigid sugar headgroups and flexible alkyl chain tail groups connected *via* an ether linkage rather than an ester linkage or an amide linkage (Faramarzi et al., 2017). Therefore, they have a wide range of applications and development in food, cosmetic, pharmaceutical industries, and scientific research (de Foresta et al., 2011; Jastrzebska et al., 2006; Ni et al., 2011; Pillion et al., 2002; Raman et al., 2006; Rifkin et al., 2011; Santonicola et al., 2008;

Published online: 4 April 2019
J Surfact Deterg (2019) **22:** 731–742

Weber and Benning, 1984; Zhang et al., 1996). They have been used in drug delivery (Ahmad et al., 2014), thermal stabilization (Ahmad et al., 2014), hydrolytic metabolism (Weber and Benning, 1984), salt tolerance (Zhang et al., 1996), formation of higher-ordered structure (Jastrzebska et al., 2006), co-immunoprecipitation (Lee et al., 2018), and structure analysis (Ni et al., 2011), as well as therapeutic adjuvants (Rifkin et al., 2011), permeation enhancers (Pillion et al., 2002), absorption enhancers (Gradauer et al., 2017), and membrane protein stabilizers against denaturation (Das et al., 2017; de Foresta et al., 2011; Jastrzebska et al., 2006; Klammt et al., 2012; Newby et al., 2009; Raman et al., 2006; Santonicola et al., 2008; Whorton and MacKinnon, 2013).

However, there are not enough data and messages available to support effectively the application in the field of life and material sciences although there are some available features/parameters including critical micelle concentration (CMC) (Frotscher et al., 2017; Matsuoka et al., 2017; Santonicola et al., 2008), sugar headgroup structure (Ehsan et al., 2016), field-induced phase transition (Hashim et al., 2017), paracellular permeation (Gradauer et al., 2017), and cell metabolism (Smułek et al., 2017). The corresponding fairly accurate and feasible screening should rely heavily on the empirical evidence, exhaustive trial-and-error process and rational thinking, and even intuitive approach. Therefore, it is still indispensable to investigate systematically the water solubility of glycosides, surface activity, and other properties to acquire the related data that are convenient for scientific research and practical applications.

Based on their bigger hydrophilic disaccharide headgroups, alkyl D-maltosides should have higher water solubility than that of alkyl D-glucosides with the same alkyl chain length. Alkyl D-maltosides with a longer alkyl chain length would improve the surface properties (for example micelle size) to a certain extent as a class of sugar-based surfactants/detergents available for the related research and applications (Smułek et al., 2017). For the α-anomer and β-anomer micelles with dodecyl group tails, the computed radii of gyration were 20.2 and 25.4 Å, respectively. Meanwhile, their computed (experimental) average thickness of the polar outer layer was 6.7 ± 0.3 Å (5.4 ± 0.1 Å) and 7.3 ± 0.4 Å (6.2 ± 0.1 Å), respectively. These values were 39.1% (50.9%) and 33.6% (43.6%) smaller than the calculated length of the maltose in its extended configuration (∼11.0 Å) owing to the partial folding of the maltose head. In contrast, their computed (experimental) surface areas were 60.3–61.1 $Å^2$ (58 $Å^2$) and 55.5–65.1 $Å^2$ (52 $Å^2$), respectively. Furthermore, the micelles containing the β-anomer had a more pronounced ellipsoidal shape than those containing the α anomer. In addition, the β-anomer was a linear conformation not only in its micellar form but also in its solvent form. It should be more suitable for the membrane protein studies than the α-anomer because the α-anomer was in a right-angle bent shape formed between the maltosyl headgroup and the alkyl tail group. The α-anomer appears to be more folded and constrained on the micelle surface, and hence it shows less solubility than the β-anomer (Abel et al., 2011).

There is some literature on alkyl D-maltosides (Ericsson et al., 2005; Kocherbitov and Söderman, 2004; Koeltzow and Urefer, 1984; Vill et al., 1989; von Minden et al., 2000). They can be prepared with $SnCl_4$ or $BF_3{\cdot}Et_2O$ as Lewis acid catalysts of the condensation reaction, but the condensation time is rather difficult to control to some extent and the yield was low for the condensation step as concurrent decomposition and serious α-anomerization take place (Aripin et al., 2012). Alkyl β-D-maltoside (Pillon et al., 2002), deuterated dodecyl β-D-maltoside (d_{39}-DDM) (Hiruma-Shimizu et al., 2014), and dodecyl β-D-melibioside (Hutchison et al., 2017) were stereoselectively prepared by the Koenigs and Knorr procedure with silver carbonate or silver triflate (AgOTf) as an expensive promoter in the coupling reaction. However, the Koenigs and Knorr procedure usually is uneconomic and/or may easily cause the accumulation of toxic heavy metal and the related environmental pollution in spite of its fairly high efficiency. Because the first article on the Schmidt's glycosylation method was published in 1980, the glycosyl trichloroacetimidates have been the most widely used glycosyl donors (Gao et al., 2016; Kinnaert et al., 2017). Their high popularity would be most likely due to two points: First, the relative ease of the donor preparation with the addition of base-catalyzed trichloroacetonitrile to the anomeric hydroxy group; and second, the high anomeric selectivity of subsequent coupling reactions *via* an eight-membered cyclic transition state (Chen and Kong, 2003; Kumar et al., 2011).

Herein, to gain more detailed insights into the structure–property relationships, we investigate the related surface properties involving solubility, foaming property, surface tension, hygroscopicity, moisture retention capacity, thermotropic liquid crystalline behavior, and skin irritation of synthetic alkyl β-D-maltosides (**6a**–**6i**, n = 6–18) (Fig. 1) with the homologous series.

Experimental Section

General Methods and Synthesis

^{1}H NMR spectra were recorded using an Avance 400 spectrometer (Bruker Daltonics Inc., Fällanden, Switzerland). Optical activities were obtained using a Perkin-Elmer model 341-MC automatic polarimeter (Perkin-Elmer, Inc., Waltham, MA). Melting points were measured using an X-4 digital melting point apparatus (Yuhua instruments Co., Ltd, Henan, China). Surface tension was determined using

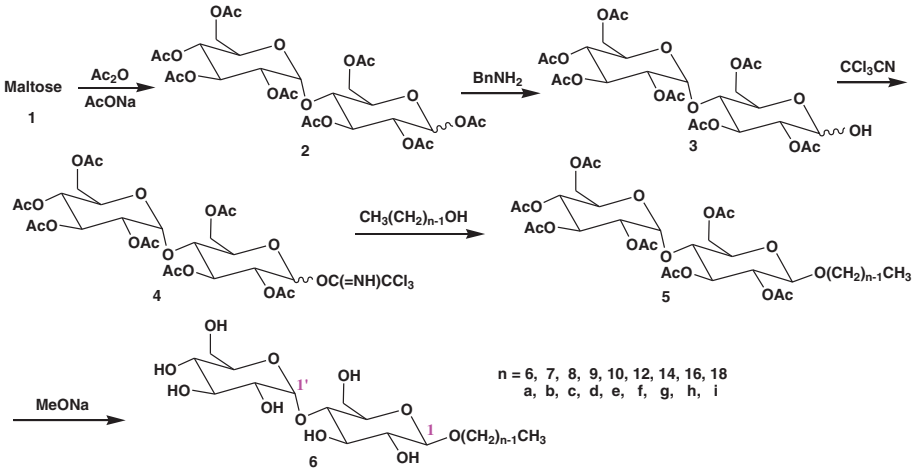

Fig. 1 Synthetic route for alkyl β-D-maltosides

a DCAT11 Tensiometer (Dataphysics Instruments Ltd, Filderstadt, Germany). Thermotropic liquid crystalline behavior was investigated using a DM-LM-P polarization microscope (Leica, Wetzlar, Germany) with a Leitz 350 hot stage. Thermal stability was determined using a TGA Q50 thermogravimetric analyzer (TA Instruments, NewCastle, DE, USA). All raw materials and solvents were of chemical grade or analytical grade.

The detailed synthetic process (Fig. 1) and the related characterization of alkyl β-D-maltosides (**6a**–**6i**, n = 6–18) were compiled in Appendix S1 (Supporting Information) according to the published glycosidation procedure (Chen et al., 2016a, 2016b; Chen and Kong, 2003).

Thermal Stability

Thermogravimetric analysis (TGA) curve was recorded for alkyl β-D-maltoside (**6a**–**6i**) under a nitrogen atmosphere at a heating rate of 20 °C min^{-1}.

Thermotropic Phase Behavior

Thermotropic liquid crystalline behavior was studied using polarization microscopy (POM) according to the literature (Chen et al., 2016a).

Hydrophilic–Lipophilic Balance (HLB) Number

The HLB number was calculated using the following methods.

Method 1: According to Griffin's method (Ji et al., 2017), the HLB number of β-D-maltoside (**6a**–**6i**) was calculated by Eq. (1):

$$HLB = 20\frac{W}{W+O} \tag{1}$$

where W is the molecular mass (341.29) of the hydrophilic sugar headgroup for β-D-maltoside (**6a**–**6i**); O is the molecular mass of the lipophilic alkyl group.

Method 2: According to Davies' group contribution method (Berger et al., 2005; Zhou et al., 2001), the HLB number was calculated by Eq. (2):

$$HLB = 7 + \Sigma(H) - \Sigma(L) \tag{2}$$

where H is the group contributions for the hydrophilic portions in the molecule, L is the contribution from the lipophilic portions in β-D-maltoside (**6a**–**6i**).

Method 3: According to the empirical relationship HLB = 60H/(H + 2) from ^{1}H NMR technology (Ben-et and Tartarsky, 1972; Zheng et al., 2007; Zhou and Cui, 2001), H is the ratio of the hydrogen atom numbers (including OH, CH, and CH_2 in the sugar ring, and OCH_2 in the alkoxy chain) to total hydrogen atom numbers. Therefore, the HLB number of β-D-maltoside (**6a**–**6i**) was obtained by Eq. (3):

$$\mathrm{HLB} = \frac{1380}{4n+67} \tag{3}$$

where n is the number of carbon atoms in the alkyl chain of β-D-maltoside (**6a**–**6i**).

Method 4: The HLB number was calculated by Eq. (4) based on the small revision of Eq. (3):

$$\mathrm{HLB} = \frac{1380}{3.4n+65.5} + 4.9\times10^{-2}(n-6) - 3.5\times10^{-4}(n-18)^2 \tag{4}$$

where n is the carbon atom numbers of the alkyl chain in β-D-maltoside (**6a**–**6i**).

Method 5: Because $H = 23/(2n + 22)$, the HLB number was calculated as shown in Eq. (5) below:

$$\mathrm{HLB} = \frac{49.110H}{H + 1.391} - \frac{0.046}{H^2} + \frac{0.797}{H} - 1.127 \quad (5)$$

where H was the same as H in Eq. (3).

Solubility

According to the literature method (Chen et al., 2016a; Ji et al., 2017), the solubility of alkyl β-D-maltoside (**6a–6i**) was determined at 25 °C in water, ethanol, and ethyl acetate, respectively.

Hygroscopicity and Moisture-Retention

According to the literature method (Chen et al., 2017; Shen et al., 2018), the hygroscopicity capacity and the moisture-retention capacity were determined using the weight method in relative humidity (RH) 81% or RH 43% at 25 °C. The results of moisture-retention capacity were compared with the capacity of glycerol.

Foaming Properties

Foaming properties were investigated using the published method (Li et al., 2016; Poole, 1989; Zhou et al., 2017). 0.25% (mass fraction) β-D-maltoside (**6a–6g**) aqueous solutions were prepared at 25 °C and then the aqueous solutions (10 mL) were transferred into the graduated cylinder (100 mL) with a plug. The solutions were followed by vigorous shaking for 1 min and the volume of the produced foam was recorded. The disappearance rate (ν) of the foams was calculated according to Eq. (6) and their stability was assessed:

$$\nu = \frac{(H_0 - H_5)}{60 \times 5} \quad (\mathrm{mL\,s^{-1}}) \quad (6)$$

where H_0 was the initial volume of the foam that was produced at the end of shaking, H_5 was the volume of the foam retained at 5 min after shaking.

Surface Tension

The surface tension (γ) of alkyl β-D-maltoside (**6a–6g**) aqueous solution was assessed using the literature method with the Wilhelmy vertical plate technique at constant temperature (25 °C). The related details are shown in Appendix S1 (Chen et al., 2016a; Shen et al., 2018; Zhang et al., 1996).

Table 1 ^{1}H NMR data of anomeric protons of alkyl β-D-maltosides

D-maltoside	solvent	H-1 δ (d/s, $J_{1,2}$)	H-1′ δ (d/s, $J_{1,2}$)
6a	D_2O	4.48 (d, 8.0 Hz)	5.42 (d, 3.6 Hz)
6b	D_2O	4.45 (d, 7.9 Hz)	5.40 (d, 3.0 Hz)
6c	D_2O	4.45 (d, 7.9 Hz)	5.39 (d, 2.8 Hz)
6d	D_2O	4.40 (d, 7.6 Hz)	5.36 (d, 2.8 Hz)
6e	D_2O	4.39 (d, 7.1 Hz)	5.36 (s)
6f	D_2O	4.37 (d, 6.4 Hz)	5.35 (s)
6g	D_2O	4.35 (d, 4.1 Hz)	5.33 (d, 1.0 Hz)
6h	DMSO-d6/D_2O	4.16 (d, 7.7 Hz)	5.03 (d, 3.4 Hz)
6i	DMSO-d6	4.14 (d, 7.7 Hz)	5.00 (d, 3.0 Hz)

Results and Discussion

Structure Confirmation

^{1}H NMR data of synthetic alkyl β-D-maltosides (**6a–6i**) are shown in Appendix S1. As shown in Table 1, the chemical shifts (the coupling constant) of anomeric protons of alkyl β-D-maltosides (**6a–6g**) are 5.33–5.42 ppm ($J_{1,2} \le 3.6$ Hz) for H-1′ and 4.35–4.48 ppm ($J_{1,2}$ 4.1–8.0 Hz) in D_2O for H-1. Meanwhile, the chemical shifts (the coupling constant) of β-D-maltoside (**6h**) are 5.03 ppm ($J_{1,2} = 3.4$ Hz) for H-1′ and 4.16 ppm ($J_{1,2} = 7.7$ Hz) for H-1 in dimethyl sulfoxide-d6/deuterium oxide (DMSO-d6/D2O). Furthermore, the chemical shifts (the coupling constant) of β-D-maltoside (**6i**) are 5.00 ppm ($J_{1,2} = 3.0$ Hz) for H-1′ and 4.14 ppm ($J_{1,2} = 7.7$ Hz) for H-1 in DMSO-d6. All data indicate that the newly formed glycosyl bond (**6a–6i**) is in a 1,2-trans β-configuration because the configuration is the 1,2-trans β-anomer as 4 Hz < $J_{1,2} \le 8$ Hz and the configuration is the 1,2-cis α-anomer as $J_{1,2} < 4$ Hz (Aripin et al., 2012; Boyd et al., 2000; Chen and Kong, 2003; Hiruma-Shimizu et al., 2014).

Thermal Stability

TGA is an important and useful method in investigating the pyrolysis behavior and assessing thermal stability. The thermal stability of alkyl β-D-maltoside was achieved by TGA at a rate of 20 °C min^{-1} under a nitrogen atmosphere as described in the Appendix S1 (Fig. S3). Alkyl β-D-maltosides (**6a–6i**) were found to show typically a first-order pyrolysis behavior. The related data are shown in Table 2. All β-D-maltosides decomposed above 220 °C, indicating that they had excellent thermal stability mainly owing to the intramolecular and multiple intermolecular H-bonding interactions of their headgroup.

Table 2 TGA data of alkyl β-D-maltosides

D-maltoside	Initial decomposition temperature (°C)	Temperature at maximum thermal decomposition velocity (°C)	Last degradation temperature (°C)	Total weight loss (%)
6a	232.2	354.7	405.8	88.7
6b	235.0	363.2	403.5	92.4
6c	228.8	359.3	409.2	94.8
6d	241.8	368.3	409.4	87.5
6e	262.8	336.0	422.1	93.5
6f	244.0	329.6	403.1	89.1
6g	258.3	340.9	409.8	90.3
6h	263.5	357.5	413.0	92.7
6i	250.2	347.1	409.0	90.1

Thermotropic Phase Behavior

For the glycosides that are composed of one aliphatic chain and one sugar group, lamellar smectic A or A* (chiral smectic A, S_A*) phases (Boyd et al., 2000; Calderer, 2001; Goodby et al., 2007; Yelamaggad et al., 2005), depending on their stereochemistry, should lead to a microphase segregation between the carbohydrate moieties and the aliphatic chains. The S_A* phase exhibits characteristic defect textures that were observed using a polarizing microscope (Goodby et al., 2007). Accordingly, alkyl β-D-maltosides (**6c**–**6i**) show only S_A* phases in their pure state. However, hexyl β-D-maltoside (**6a**) and heptyl β-D-maltoside (**6b**) did not show distinctive A* phases because both glycosides perhaps had shorter alkyl chains so as to do not effectively form distinctive S_A* phases. The thermotropic phase behavior of β-D-maltosides (**6c**–**6i**) was characterized by polarizing microscopy and the data are shown in the Appendix S1 (Fig. S2).

The double melting transition temperatures of alkyl *D*-maltosides (**6a**–**6i**) are summarized in Table 3. D-maltosides (**6c**–**6i**) possessed sharp melting temperatures (T_{lc}, transition temperature from the crystallized solid into a liquid crystal) and sharp clearing temperatures (T_{iso}, transition temperature from a liquid crystal into an isotropic liquid). The mesophase temperature ranges ($\Delta T = T_{iso} - T_{lc}$) of alkyl D-maltosides (**6c**–**6g**) increased with increasing the alkyl chain length. For hexadecyl D-maltoside (**6h**) and octadecyl D-maltoside (**6i**), their mesophase temperature ranges were near each other because they had almost the same T_{lc} and T_{iso} values and reached a plateau where there would be an optimal balance between the hydrophilic part and hydrophobic part of the liquid crystal.

Such an optical observation of the so-called double melting points in amphiphilic sugar-based surfactants was also reported in the literature (Boyd et al., 2000; Ericsson et al., 2005). Many researchers (Boyd et al., 2000; Ericsson et al., 2005; Kocherbitov and Söderman, 2004; Koeltzow and Urefer, 1984; Vill et al., 1989; von Minden et al., 2000; Wang and Zhang, 2017) found similar data on D-maltosides (Table 3). However, Bonicelli et al. (1998) observed that decyl D-maltoside (**6e**) had a pretransition at 78.6 °C and a solid–liquid crystal phase transition at 96.5 °C. Finally, the mesophase behavior of maltosides is yet not fully understood in spite of a large amount of experimental data. Instead, there is no doubt that other techniques such as differential scanning calorimeter, X-ray diffraction, TGA, small-angle X-ray scattering, wide-angle X-ray scattering, deuterium NMR, fourier transform infrared spectroscopy, and small-angle neutron scattering should be used to elucidate their complex mesophase information in the future.

Table 3 Phase transition temperatures of alkyl β-D-maltosides

maltoside	R	T_{lc}/°C	T_{iso}/°C	ΔT/°C
6a	n-C_6H_{13}	—	—	—
6b	n-C_7H_{15}	—	—	—
6c	n-C_8H_{17}	86.2 (54[a]; 89–103[b])	118.0 (122.7[a]; 125[b])	31.8
6d	n-C_9H_{19}	83.2	124.7	41.5
6e	n-$C_{10}H_{21}$	86.4 (58[a]; 96–100[b]; 86[c])	126.5 (205.9[a]; 207–208[b]; 156–159[c])	50.1
6f	n-$C_{12}H_{25}$	94.5 (95–105[b]; 76–76.5[c]; 102[d]; 65[e]; 102[f])	241.0 (245[b]; 125–127[c]; 244[d]; 244[e]; 245[f])	146.5
6g	n-$C_{14}H_{29}$	97.4 (107[f])	248.3 (264[f])	150.9
6h	n-$C_{16}H_{33}$	98.9	259.0	160.1
6i	n-$C_{18}H_{37}$	100.2 (76–91[c]; 106[f])	260.6 (188–210[c]; 274[f])	160.4

[a] Kocherbitov and Söderman, 2004.
[b] Boyd et al., 2000.
[c] Koeltzow and Urefer, 1984.
[d] Vill et al., 1989.
[e] Ericsson et al., 2005.
[f] von Minden et al., 2000.

HLB Number, Partition Coefficient, and Solubility

The HLB number, as an empirical parameter that was introduced by William C. Griffin in 1949, was originally developed as a scale to classify the relative effectiveness of nonionic surfactants at forming stable emulsions at room temperature. To date, it is one of the most significant properties of a surfactant.

Table 4 HLB number and water solubility (g per 100 g) of alkyl D-maltoside

D-maltoside	**6a**, C6	**6b**, C7	**6c**, C8	**6d**, C9	**6e**, C10	**6f**, C12	**6g**, C14	**6h**, C16	**6i**, C18
HLB number (by Eq. (1))	16.01	15.50	15.02	14.57	14.14	13.37	12.67	12.04	11.48
HLB number (by Eq. (2))	16.95	16.48	16.00	15.53	15.05	14.10	13.15	12.20	11.25
HLB number (by Eq. (3))	15.16	14.53	13.94	13.40	12.90	12.00	11.22	10.53	9.93
HLB number (by Eq. (4))	16.01	15.46	14.95	14.48	14.04	13.26	12.59	12.00	11.48
HLB number (by Eq. (5))	16.02	15.46	14.95	14.48	14.05	13.27	12.59	12.00	11.48
Difference (Eq(1)-Eq(3))	0.85	0.97	1.08	1.17	1.24	1.37	1.45	1.51	1.55
Difference (Eq(1)-Eq(4))	0	0.04	0.07	0.09	0.10	0.11	0.08	0.04	0
Difference (Eq(1)-Eq(5))	−0.01	0.04	0.07	0.09	0.09	0.10	0.08	0.04	0
log*P*	−1.68	−1.24	−0.85	−0.43	−0.01	0.82	1.66	2.49	3.33
Water solubility	69.31	55.06	38.36	33.17	15.23	7.04	0.78	0.0012	0

There are several methods including obtaining the HLB number (Ben-et and Tartarsky, 1972; Berger et al., 2005; Ji et al., 2017; Zheng et al., 2007; Zhou et al., 2001; Zhou and Cui, 2001). Table 4 and Fig. 2 show the HLB numbers from Eq. (1), Eq. (2), and Eq. (3), respectively. HLB numbers decrease with increasing alkyl chain length in the range of C6–C18. However, the HLB number (by Eq. (3)) was smaller than the HLB numbers (by Eq. (1) and by Eq. (2)) for the same alkyl chain length.

In Table 4 and Fig. 2, the HLB numbers in Eq. (3) are very far away from the values calculated from Eq. (1). When Eq. (4) is applied, diifferences are reduced (Table 4). Note that HLB numbers in both Eq. (3) and Eq. (4) are a function of alkyl chain length (n) in *β-D*-maltoside (**6a–6i**)).

Next, we expected to obtain further information directly from the related ^{1}H NMR spectra and/or the molecular structures. For β-D-maltoside (**6a–6i**), we found relationships between the chemical shift (δ) and the alkyl chain length (n) as follows: (i) δ < 2.50 ppm for the $(CH_2)_{n\text{-}2}CH_3$) part of $OCH_2(CH_2)_{n\text{-}2}CH_3$; (ii) δ > 2.50 ppm for both OH, CH, and CH_2 in the sugar ring and the OCH_2 part of $OCH_2(CH_2)_{n\text{-}2}CH_3$ in the alkoxy group. In the ^{1}H NMR spectrum, the related integrated values of the hydrogen atom were counted as 23 for δ > 2.50 ppm in *β-D*-maltoside (**6a–6i**). Therefore, $H = 23/(2n + 22)$ where H is the ratio of particular hydrogen atom numbers (including OH, CH, and CH_2 in the sugar ring, and OCH_2 in the alkoxy chain) to the total hydrogen atom numbers in β-D-maltoside (**6a–6i**). Finally, Eq. (5) was readily obtained from $H = 23/(2n + 22)$ and Eq. (4) because the H values can be actually obtained from the related the ^{1}H NMR spectra and/or the molecular structures.

Herein, DMSO-d6 was used as the ^{1}H NMR deuterated solvent because of the chemical shifts (δ, ppm) (5.49 (1H), 5.45 (1H), 5.06 (1H), 4.90 (2H), 4.51 (1H), and 4.46 (1H)) of all OH in octadecyl β-D-maltoside (**6i**). As an example, it can be just discovered near the chemical shifts (δ, ppm) (4.14 (H-1) and 5.00(H-1′) of both anomeric hydrogens of the sugar headgroup at a high chemical shift ($\delta \geq 4.0$ ppm) (Ben-et and Tartarsky, 1972). For any mixture of alkyl D-maltoside (n = 6–18) with different alkyl chain lengths and ratios, the corresponding HLB number should be readily achieved with DMSO-d6 as a deuterated solvent in ^{1}H NMR experiment.

In fact, some hydrogen atoms (including CH and CH_2 in the sugar ring, and the OCH_2 part of $OCH_2(CH_2)_{n\text{-}2}CH_3$ in the alkoxy group) were just in the range of δ = 2.9–5.5 ppm in spite of a lower chemical shift (δ < 2.5 ppm) for $(CH_2)_{n\text{-}2}CH_3$) of $OCH_2(CH_2)_{n\text{-}2}CH_3$ in various deuterated solvents such as D_2O, DMSO-d6, and DMSO-d6/D_2O (Zheng et al., 2007). Therefore, Eq. (5) indeed provided effective access to obtain the HLB number from the molecular structure and/or the data of the related ^{1}H NMR spectrum.

Figure 3 shows the solubility of alkyl β-D-maltosides (**6a–6i**) at 25 °C in water, ethanol, and ethyl acetate, respectively. The maltosyl headgroup of alkyl β-D-maltoside not only has strong intermolecular hydrogen bonds (inter-HB) in water, which increases water solubility, but also has strong and rather stable intramolecular hydrogen bonds (intra-HB)

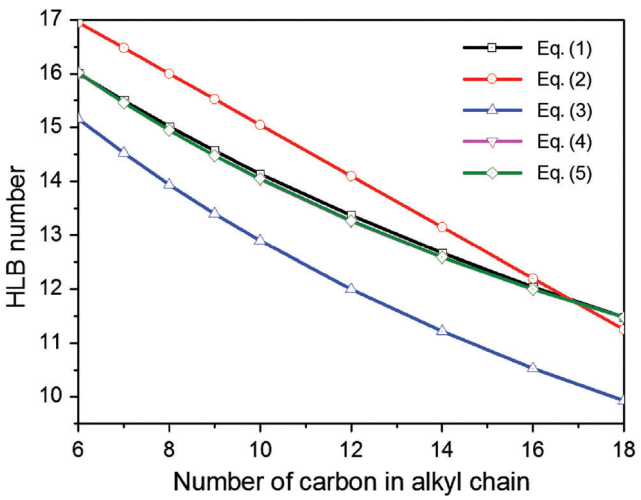

Fig. 2 HLB numbers of alkyl β-D-maltosides

that may somewhat weaken the inter-HB. The alkyl chain tail group is a hydrophobic group and, therefore, has an opposite effect on water solubility. As shown in Fig. 3 and Table 4, water solubility decreased rapidly with increasing alkyl chain length. Finally, two of the *β-D*-maltosides, (**6h** (n = 16) and **6i** (n = 18)), were water insoluble.

In contrast, the solubility in ethanol, at first, increased with increasing alkyl chain length for $n \leq 10$, then reached the maximum value for n = 10 and subsequently decreased with increasing alkyl chain length for $n > 10$. Nonetheless, all β-D-maltoside (**6a–6i**) did not dissolve in ethyl acetate for n = 6–18.

The octanol–water partition coefficient value (log*P*) of alkyl β-D-maltoside (**6a–6i**) was calculated by ChemBiodraw (Ultra 14.0), as shown in Table 4.

HLB numbers and the log*P* values of alkyl *β-D*-maltosides (**6a–6g**) were within the range of 12.67–16.01 (Eq. (1)) and − 1.68–1.66, respectively (Table 4), which illustrate that they have stronger hydrophilicity and could be used to stabilize O/W emulsions. However, the HLB numbers and the log*P* values of alkyl β-D-maltosides (**6h** and **6i**) were in the range of 11.48–12.04 (Eq. (1)) and 2.49–3.33, respectively. Such glycosides are considered to have weaker hydrophilicity although they should perhaps have the ability to stabilize O/W emulsions to some extent because their HLB number was bigger than 10.

The literature (Berger et al., 2005) indicates that surfactants with HLB numbers between 10 and 20 are water-soluble and generally form stable, oil-in-water (O/W) emulsions, whereas surfactants with HLB numbers below 10 are oil-soluble and generally form water-in-oil (W/O) emulsion. Thus, the nonionic amphiphilic surfactants, *β-D*-maltosides (**6a–6i**), probably are, therefore, suitable as O/W emulsifiers because their HLB numbers are in the range of 10–17.

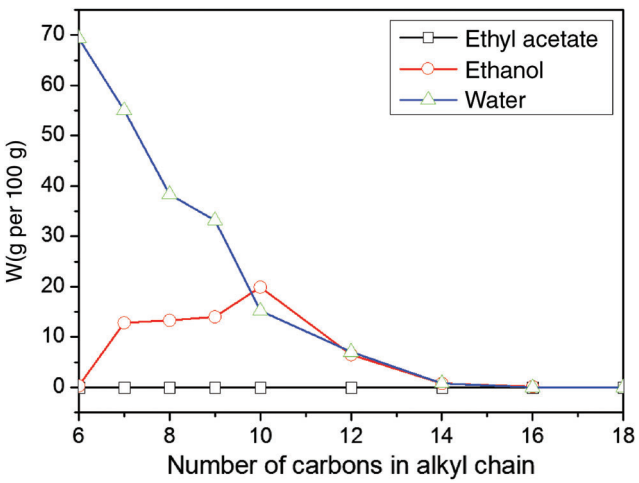

Fig. 3 Solubility of maltosides in ethyl acetate, ethanol, and water

In this sense, the HLB numbers from Eq. (4) and Eq. (5) should also be reasonable. Table 4 shows that the maltosides (**6a–6g**) are water-soluble and their HLB numbers are bigger than 12.50, whereas the maltosides (**6h** and **6i**) have poor water solubility and their HLB numbers are within the range of 11.5–12. In fact, hexadecyl β-D-maltoside (**6h**, n = 16) is almost water insoluble (only 0.0012 g per 100 g (water), a value that is smaller than the common threshold (0.1 g per 100 g (water)). Octadecyl β-D-maltoside (**6i**, n = 18) is completely insoluble in water.

Hygroscopicity

The hygroscopicities of alkyl β-D-maltoside (**6a–6i**) were determined with different humidity (RH43 and RH81%) at 25 °C. The results are shown in Fig. 4. The experiments show that the hygroscopicity (R_h) value increases with time, but decreases with increasing alkyl chain length. The R_h value reaches a maximum value at 48 h. The R_h value at RH43% was bigger than that at RH81%. The R_h value of dodecyl β-D-maltoside (**6f**) reaches 14.8% (RH81%) and 23.2% (RH43%), respectively, at 48 h mainly attributed to the intermolecular H-bonding network of its polyhydroxy group in water.

Moisture-Retention Capacity

β-D-maltosides (**6a–6e**) and glycerol were selected to investigate their moisture-retention capacity (R_m), and the results are shown in Fig. 5. R_m values of glycerol decrease with the time, and also decreased faster at RH81% than that at RH43%. The decreasing tendency of R_m values of *D*-maltosides (**6a–6e**) is similar to that of glycerol at RH43% and at RH81%. The R_m value of D-maltoside (**6a–6e**) decreases with increasing alkyl chain length. The R_m values of D-maltosides (**6a–6e**) at RH81% are smaller and decrease faster than at RH43%.

Foaming Properties

The foaming behavior of alkyl β-D-maltoside (**6a–6g**) aqueous solutions was evaluated at 25 °C, and the results are presented in Fig. 6. The initial foam volume (H_0) increases with the alkyl chain length for $n \leq 9$. Nonyl β-D-maltoside (**6d**, n = 9) shows the strongest foaming power (H_0). However, the H_0 value subsequently decreased with increasing alkyl chain length for $n > 9$. The volume (H_5) of the foam retained at 5 min after shaking was high, for n = 9–12, but decreased for $n < 9$ and $n > 12$. The disappearance rate (ν) of the foam decreased with increasing alkyl chain length for $6 \leq n \leq 14$. The smaller the disappearance rate (ν) of foam, the higher the foam stability. The disappearance rate (ν) was almost equal to zero for tetradecyl β-D-maltoside (**6g**, n = 14), meaning high foam

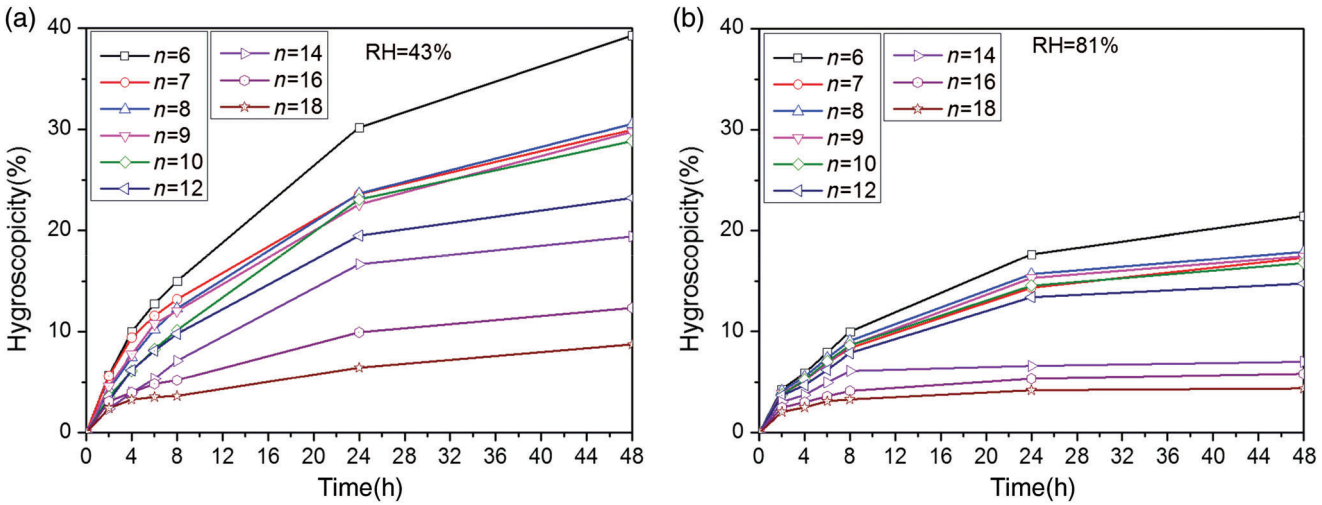

Fig. 4 Hygroscopicity (R_h) of D-maltosides **(a)** RH = 43%; **(b)** RH = 81%

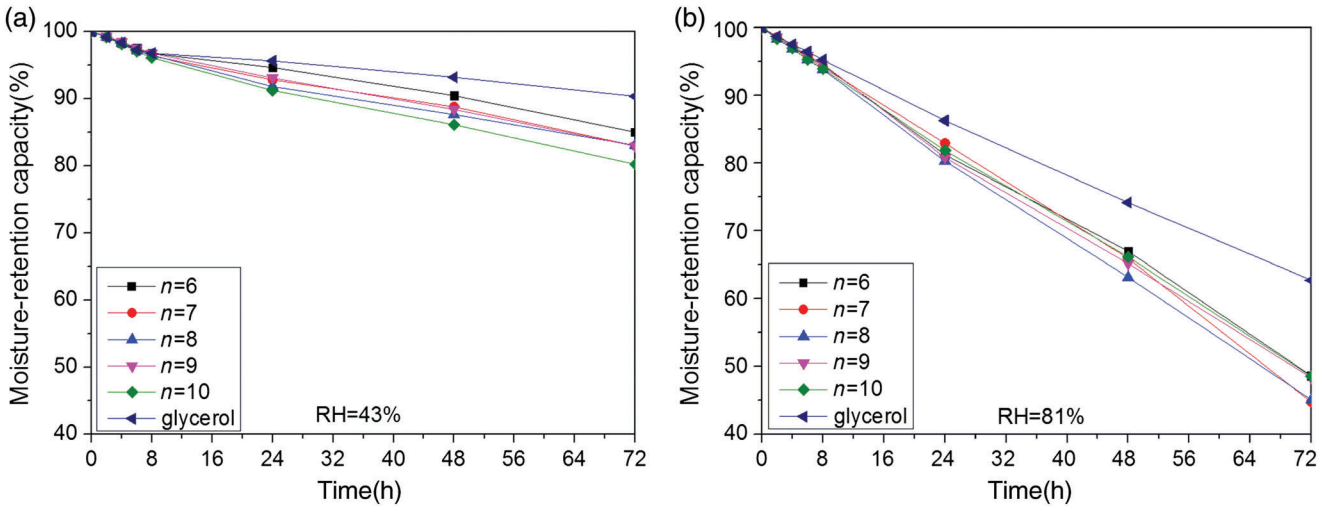

Fig. 5 Moisture-retention capacity (R_m) of D-maltosides and glycerol **(a)** RH = 43% (left); **(b)** RH = 81% (right)

stability. In a practical way, nonyl β-D-maltoside (**6d**, n = 9), decyl β-D-maltoside (**6e**, n = 10), and dodecyl β-D-maltoside (**6f**, n = 12) should be considered as good foaming agents as they showed the highest foaming power and better stability.

Surface Tension

Figure 7 shows the relationship between the surface tension (γ) of alkyl β-D-maltoside (**6a**–**6g**) and the logarithm of the concentration (C). The corresponding CMC and γ_{CMC} (surface tension at CMC) obtained from Fig.7 are presented in Table 5.

CMC and γ_{CMC} values decrease with increasing alkyl chain length. Accordingly, tetradecyl *β-D*-maltoside (**6g**) shows the lowest CMC and γ_{CMC} values.

Table 5 also shows the surface excess concentration (Γ_{max}) and the minimum area (A_{min}) data. The Γ_{max} value of alkyl β-D-maltoside (**6a**–**6g**) decreases slowly with increasing alkyl chain length. A_{min} values increase slightly with increasing alkyl chain length. Indeed, the longer the hydrophobic alkyl chain length, the bigger A_{min}, and the smaller Γ_{max}.

Furthermore, the values of effectiveness (π_{CMC}) were obtained with Eq. (S5) in Appendix S1 and are listed in Table 5. The π_{CMC} value increases with increasing hydrophobic chain length. Accordingly, the π_{CMC} value is the highest (38.16 mN m^{-1}) for tetradecyl β-D-maltoside (**6g**), and, therefore, it shows the best ability to decrease surface tension.

In addition, Table 5 also provides the efficiency (pC_{20}) data obtained from Eq. (S6) in Appendix S1. The pC_{20} value of

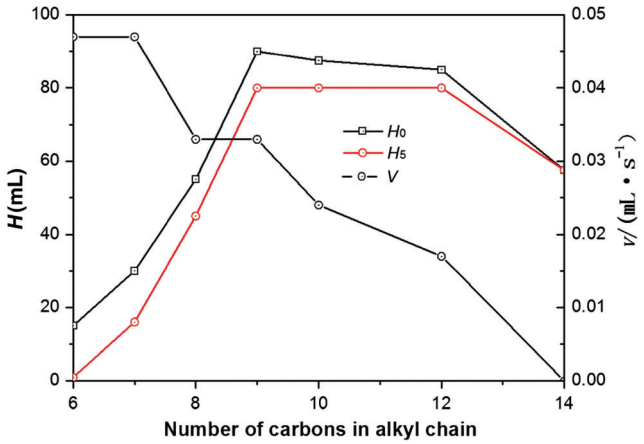

Fig. 6 Foaming ability of alkyl D-maltosides

hexyl β-D-maltoside (**6a**) was only 2.14 mol L^{-1}, suggesting that its efficiency was the lowest. The pC_{20} value increased gradually with increasing alkyl chain length, so that the efficiency of tetradecyl β-D-maltoside (**6g**) should be the highest.

The standard free energy of micellization (ΔG_{mic}) and the standard free energy of adsorption (ΔG_{ads}) values of D-maltosides (**6a**–**6g**) are negative as shown in Table 5. Their ΔG_{mic} and the ΔG_{ads} values became gradually more negative with increasing alkyl chain length. Because the alkyl chains of the D-maltosides are hydrophobic, the entropic effect is the most important contribution to the overall Gibbs free energy of aggregation. Because ΔG_{ads} values are more negative than ΔG_{mic} for the same alkyl chain, adsorption at the air/water interface appears to be more favorable than the micellization in solution.

Ogawa's group (Ogawa et al., 2013) investigated the surface activities of a series of alkyl β-*g*lucopyranosides (n = 5–10) (Table6). For n = 6–8, the CMC values of maltosides are smaller than the critical aggregation concentration values of glucosides with the same alkyl chain length; For n = 9 and 10, the CMC values of maltosides are greater than the CAC values of glucosides with the same alkyl chain length. All surface tension values at the CMC (γ_{CMC}) of alkyl maltoside are greater than surface tension values at the CAC (γ_{CAC}) value of glucoside with the same alkyl chain length. The A_{min} value of maltoside increases with increasing alkyl chain length, but the change of the A_{min} value of alkyl glucoside shows no definite trend with increasing alkyl chain length.

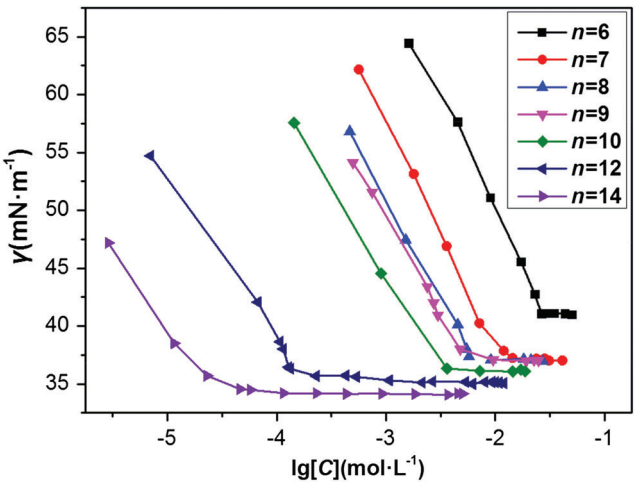

Fig. 7 Surface tension of aqueous alkyl D-maltoside solution

Acute Skin Irritation

Alkyl β-D-maltosides (**6a**–**6g**) were tested for acute skin irritation including erythema, edema at 1, 24, and 48 h on mice. The corresponding stimulating effects on the local skin were summarized according to the scoring system (i.e., the experimental mean score 0–0.4 was classified as the non-irritation reaction, 0.5–1.9 was light stimulation, 2.0–5.9 was moderate stimulation, and 6.0–8.0 was strong stimulation) (British Standard Institution, 2010; General Administration of Quality Supervision, Inspection and Quarantine of P.R.C., 2000). The experimental results are shown in Appendix S1 (Table S1). The total scores were as low as 0.1, which is classified as the nonirritation reaction. Therefore, alkyl *β-D*-maltosides (**6a**–**6g**) produce no skin irritation, and they should be considered as safe sugar-based surfactants.

Conclusion

Alkyl β-D-maltosides (**6a**–**6i**, n = 6–18) are nonionic amphiphilic disaccharide-based surfactants. To validate their potential application, their structure–property relationships were investigated. Their calculated HLB number and water solubility at 25 °C decrease with increasing alkyl chain length. Their hygroscopicity and moisture retention capacity also decrease gradually with increasing alkyl chain length. Hexyl β-D-maltoside (**6a**) and heptyl β-D-maltoside (**6b**) have good moisture retention capacity. Decyl β-D-maltoside (**6e**) and dodecyl β-D-maltoside (**6f**) have outstanding foaming power and foaming stability. Alkyl β-D-maltosides (**6a**–**6g**) have excellent surface activity. The CMC, γ_{CMC}, and the Γ_{max} values decrease monotonously with increasing alkyl chain length. A_{min}, π_{CMC}, and the pC_{20} values increase gradually with alkyl chain length. ΔG_{mic} and ΔG_{ads} become more negative with increasing alkyl chain length. Furthermore, the ΔG_{ads} values are more negative than ΔG_{mic} for the same alkyl chain length. Concerning thermotropic behavior, a distinctive thermotropic A* phase for β-D-maltoside (**6c**–**6i**) was found. The melting temperature, the clearing temperature, and the

Table 5 Adsorption parameters of alkyl D-maltoside

D-maltoside	CMC (mol L^{-1})	γ_{CMC} (mN m^{-1})	$\Gamma_{max} \times 10^{10}$ (mol cm^{-2})	A_{min} (Å^2)	π_{CMC} (mN m^{-1})	pC_{20} (mol L^{-1})	ΔG_{mic} (kJ mol^{-1})	ΔG_{ads} (kJ mol^{-1})
6a	2.86×10^{-2}	41.15	3.43	48.36	31.45	2.14	−8.66	−17.83
6b	1.16×10^{-2}	37.34	3.36	49.39	35.26	2.74	−10.86	−21.35
6c	6.18×10^{-3}	37.15	3.18	52.24	35.45	3.06	−12.39	−23.54
6d	5.26×10^{-3}	37.08	2.99	55.56	35.52	3.20	−12.79	−24.67
6e	2.91×10^{-3}	36.26	2.74	60.63	36.34	3.59	−14.23	−27.49
6f	2.00×10^{-4}	35.28	2.50	66.45	37.32	4.98	−20.75	−35.68
6g	2.66×10^{-5}	34.44	2.30	72.23	38.16	5.97	−25.67	−42.26

Table 6 Adsorption parameters of alkyl β-D-maltoside and alkyl β-D-glucopyranoside

β-D-glucoside (n)	CAC (mol L^{-1})	γ_{CAC} (mN m^{-1})	A_{min} (Å^2)	β-D-maltoside (n)	CMC (mol L^{-1})	γ_{CMC} (mN m^{-1})	A_{min} (Å^2)
C_5Glc (n = 5)	5.316×10^{-1}	38.1	63.2				
C_6Glc (n = 6)	2.322×10^{-1}	34.4	49.4	**6a (n = 6)**	2.86×10^{-2}	41.15	48.36
C_7Glc (n = 7)	5.93×10^{-2}	32.0	45.0	**6b (n = 7)**	1.16×10^{-2}	37.34	49.39
C_8Glc (n = 8)	1.46×10^{-2}	29.6	47.9	**6c (n = 8)**	6.18×10^{-3}	37.15	52.24
C_9Glc (n = 9)	5.0×10^{-3}	29.0	44.3	**6d (n = 9)**	5.26×10^{-3}	37.08	55.56
C_{10}Glc (n = 10)	1.3×10^{-3}	28.0	48.4	**6e (n = 10)**	2.91×10^{-3}	36.26	60.63
				6f (n = 12)	2.00×10^{-4}	35.28	66.45
				6g (n = 14)	2.66×10^{-5}	34.44	72.23

mesophase temperature ranges of D-maltosides (**6c–6g**) increase with alkyl chain length.

Overall, this study showed that the alkyl β-D-maltosides (**6a–6i**, n = 6–18) obtained are safe, amphiphilic, and surface active. Because their maltosyl headgroup is bigger than the glucosyl headgroup of alkyl D-glucopyranoside, their solubilities are higher than that of alkyl D-glucopyranosides with the same alkyl chain length. The experimental results are expected to provide the scientific basis and are useful reference. The obtained products are expected to have potential applications in a wide variety of fields, as detergents, fine chemicals, cosmetics, food additives, and pharmaceutical products, as well as in biochemistry research and supramolecular research.

Acknowledgements This work was supported by the National Natural Science Foundation of China (Grant No. 21643010), Hunan 2011 Collaborative Innovation Center of Chemical Engineering & Technology with Environmental Benignity and Effective Resource Utilization, and the Natural Science Foundation of Hunan Province, China (Grant No. 14JJ2067).

Conflict of Interest The authors declare that they have no conflict of interest.

References

Abel, S., Dupradeau, F.-Y., Raman, E. P., MacKerell, A. D., & Marchi, M. (2011) Molecular simulations of dodecyl-β-maltoside micelles in water: Influence of the headgroup conformation and force field parameters. *Journal of Physical Chemistry B*, **115**: 487–499.

Ahmad, N., Ramsch, R., Llinàs, M., Solans, C., Hashim, R., & Tajuddin, H. A. (2014) Influence of nonionic branched-chain alkyl glycosides on a model nano-emulsion for drug delivery systems. *Colloids and Surfaces B: Biointerfaces*, **115**:267–274.

Aripin, N. F. K., Park, J. W., & Park, H. J. (2012) Preparation of vesicle drug carrier from palm oil- and palm kernel oil-based glycosides. *Colloids and Surfaces B: Biointerfaces*, **95**:144–153.

Ben-et, G., & Tartarsky, D. (1972) Application of NMR for the determination of HLB values of nonionic surfactants. *Journal of American Oil Chemistry Society*, **49**:499–500.

Berger, B. W., García, R. Y., Lenhoff, A. M., Kaler, E. W., & Robinson, C. R. (2005) Relating surfactant properties to activity and solubilization of the human adenosine A_3 receptor. *Biophysical Journal*, **89**:452–464.

Bonicelli, M. G., Ceccaroni, G. F., & Mesa, C. L. (1998) Lyotropic and thermotropic behavior of alkylglucosides and related compounds. *Colloid and Polymer Science*, **276**:109–116.

Boyd, B. J., Drummond, C. J., Krodkiewska, I., & Grieser, F. (2000) How chain length, headgroup polymerization, and anomeric configuration govern the thermotropic and lyotropic liquid crystalline phase behavior and the air-water interfacial adsorption of glucose-based surfactants. *Langmuir*, **16**:7359–7367.

British Standard Institution (BSI) (2010) *Biological evaluation of medical devices part 10: Tests for irritation and skin sensitization (ISO 10993-10:2010)*. Author. Retrieved from https://www.iso.org/standard/40884.html.

Calderer, M. C. (2001) Studies of layering and chirality of smectic a* liquid crystals. *Mathematical and Computer Modelling*, **34**: 1273–1288.

Chen, G., Li, Z., Chen, L., Ji, S., & Shen, W. (2016a) Synthesis and properties of alkyl β-D-Galactopyranoside.*Journal of Surfactants and Detergents*, **19**:1095–1105.

Chen, G., Li, Z., Chen, L., Ji, S., & Shen, W. (2017) Synthesis and properties of alkyl α-D-galactopyranoside. *Journal of Dispersion Science and Technology*, **38**:506–514.

Chen, L., & Kong, F. (2003) Unusual α-glycosylation with galactosyl donors with a C2 ester capable of neighboring group participation. *Tetrahedron Letters*, **44**:3691–3695.

Chen, L., Shen, W., Kuang, N., & Ji, S. (2016b) Synthesis of hexadecyl β-D-xylopyranoside. *Journal of Xuzhou Institute of Technology*, **31**:10–14 (in Chinese).

Das, M., Du, Y., Ribeiro, O., Hariharan, P., Mortensen, J. S., Patra, D., … Chae, P. S. (2017) Conformationally preorganized diastereomeric norbornane-based maltosides for membrane protein study: Implications of detergent kink for micellar properties. *Journal of the American Chemical Society*, **139**:3072–3081.

de Foresta, B., Vincent, M., Garrigos, M., & Gallay, J. (2011) Transverse and tangential orientation of predicted transmembrane fragments 4 and 10 from the human multidrug resistance protein (hMRP1/ABCC1) in membrane mimic. *European Biophysics Journal*, **40**:1043–1060.

Ehsan, M., Du, Y., Scull, N. J., Tikhonova, E., Tarrasch, J., Mortensen, J. S., … Chae, P. S. (2016) Highly branched penta-saccharide-bearing amphiphiles for membrane protein studies. *Journal of the American Chemical Society*, **138**:3789–3796.

Ericsson, C. A., Ericsson, L. C., & Ulvenlund, S. (2005) Solid-state phase behaviour of dodecylglycosides.*Carbohydrate Research*, **340**:1529–1537.

Faramarzi, S., Bonnett, B., Scaggs, C. A., Hoffmaster, A., Grodi, D., Harvey, E., & Mertz, B. (2017) Molecular dynamics simulations as a tool for accurate determination of surfactant micelle properties. *Langmuir*, **33**:9934–9943.

Frotscher, E., Höring, J., Durand, G., Vargas, C., & Keller, S. (2017) Model-free analysis of critical micellar concentrations for detecting demixing in surfactant mixtures.*Analytical Chemistry*, **89**: 3245–3249.

Gao, P.-C., Zhu, S.-Y., Cao, H., & Yang, J.-S. (2016) Total synthesis of marine glycosphingolipid vesparioside B. *Journal of the American Chemical Society*, **138**:1684–1688.

General Administration of Quality Supervision, Inspection and Quarantine of P.R.C. (2000) GB/T16886.10—2000 idt ISO 10993-10: 1995 Biological evaluation of medical devices—Part 10: Tests for irritation and skin sensitization (in Chinese). Retrieved from http://www.168i.cn/soft/show.asp?id=237589.

Goodby, J. W., Görtz, V., Cowling, S. J., Mackenzie, G., Martin, P., Plusquellec, D., … Fitremann, J. (2007) Thermotropic liquid crystalline glycolipids. *Chemical Society Reviews*, **36**:1971–2032.

Gradauer, K., Iida, M., Watari, A., Kataoka, M., Yamashita, S., Kondoh, M., & Buckley, S. T. (2017) Dodecylmaltoside modulates bicellular tight junction contacts to promote enhanced permeability. *Molecular Pharmaceutics*, **14**:4734–4740.

Hashim, R., Sugimura, A., Nguan, H.-S., Rahman, M., & Zimmermann, H. (2017) Anhydrous octyl-glucoside phase transition from lamellar to isotropic induced by electric and magnetic fields. *The Journal of Chemical Physics*, **146**:084702.

Hiruma-Shimizu, K., Kalverda, A. P., Henderson, P. J. F., Homans, S. W., & Patching, S. G. (2014) Synthesis of uniformly deuterated n-dodecyl-β-D-maltoside (d_{39}-DDM) for solubilization of membrane proteins in TROSY NMR experiments. *Journal of Labelled Compounds and Radiopharmaceuticals*, **57**:737–743.

Hutchison, J. M., Lu, Z., Li, G. C., Travis, B., Mittal, R., Deatherage, C. L., & Sanders, C. R. (2017) Dodecyl-β-melibioside detergent micelles as a medium for membrane proteins. *Biochemistry*, **56**:5481–5484.

Jastrzebska, B., Fotiadis, D., Jang, G.-F., Stenkamp, R. E., Engel, A., & Palczewski, K. (2006) Functional and structural characterization of rhodopsin oligomers. *The Journal of Biological Chemistry*, **281**:11917–11922.

Ji, S., Shen, W., Chen, L., Zhang, Y., & Wu, X. (2017) Synthesis and properties of alkoxyethyl 2-acetamido-2-deoxy-α-D-glucopyranoside. *Journal of Molecular Liquids*, **242**:1169–1175.

Karam, A., Vigier, K. D. O., Marinkovic, S., Estrine, B., Oldani, C., & Jérôme, F. (2017) Conversion of cellulose into amphiphilic alkyl glycosides catalyzed by Aquivion, a perfluorosulfonic acid polymer. *ChemSusChem*, **10**:3604–3610.

Kinnaert, C., Daugaard, M., Nami, F., & Clausen, M. H. (2017) Chemical synthesis of oligosaccharides related to the cell walls of plants and algae. *Chemical Reviews*, **117**:11337–11405.

Klammt, C., Maslennikov, I., Bayrhuber, M., Eichmann, C., Vajpai, N., Chiu, E. J. C., … Choe, S. (2012) Facile backbone structure determination of human membrane proteins by NMR spectroscopy. *Nature Methods*, **9**:834–839.

Kocherbitov, V., & Söderman, O. (2004) Glassy crystalline state and water sorption of alkyl maltosides. *Langmuir*, **20**:3056–3061.

Koeltzow, D. E., & Urefer, A. D. (1984) Preparation and properties of pure alkyl glucosides, maltosides and maltotriosides. *Journal of American Oil Chemistry Society*, **61**:1651–1655.

Kumar, A., Kumar, V., Dere, R. T., & Schmidt, R. R. (2011) Glycoside bond formation via acid-base catalysis. *Organic Letters*, **13**: 3612–3615.

Lee, Y.-C., Bååth, J. A., Bastle, R. M., Bhattacharjee, S., Cantoria, M. J., Dornan, M., … Lin, S.-H. (2018) Impact of detergents on membrane protein complex isolation. *Journal of Proteome Research*, **17**:348–358.

Li, Z., Chen, G., Chen, L., Shen, W., & Ji, S. (2016) Synthesis and properties of alkyl α-D-glucopyranosides. *Chinese Journal of Applied Chemistry*, **33**:1265–1273 (in Chinese).

Matsuoka, K., Miyajima, R., & Karasawa, S. (2017) Aggregate formation of glycyrrhetic acid 3-O-glucuronide. *Journal of Surfactants and Detergents*, **20**:1153–1159.

Newby, Z. E. R., O'Connell III, J. D., Gruswitz, F., Hays, F. A., Harries, W. E. C., Harwood, I. M., … Stroud, R. M. (2009) A general protocol for the crystallization of membrane proteins for X-ray structural investigation. *Nature Protocols*, **4**:619–637.

Ni, D. Q., Zook, J., Klewer, D. A., Nieman, R. A., Soll, J., & Fromme, P. (2011) Isolation, folding and structural investigations of the amino acid transporter OEP16. *Protein Expression and Purification*, **80**:157–168.

Ogawa, S., Asakura, K., & Osanai, S. (2013) Thermotropic and glass transition behaviors of n-alkyl β-D-glucosides. *RSC Advances*, **3**: 21439–21446.

Pillion, D. J., Ahsan, F., Arnold, J. J., Balusubramanian, B. M., Piraner, O., & Meezan, E. (2002) Synthetic long-chain alkyl maltosides and alkyl sucrose esters as enhancers of nasal insulin absorption. *Journal of Pharmaceutical Sciences*, **91**:1456–1462.

Poole, S. (1989) The foam-enhancing properties of basic biopolymers. *International Journal of Food Science and Technology*, **24**: 121–137.

Raman, P., Cherezov, V., & Caffrey, M. (2006) The membrane protein data bank. *Cellular and Molecular Life Sciences*, **63**:36–51.

Rifkin, R. A., Maggio, E. T., Dike, S., Kerr, D. A., & Levy, M. (2011) N-dodecyl-β-D-maltoside inhibits aggregation of human interferon-β-1b and reduces its immunogenicity. *Journal of Neuroimmune Pharmacology*, **6**:158–162.

Santonicola, M. G., Lenhoff, A. M., & Kaler, E. W. (2008) Binding of alkyl polyglucoside surfactants to bacteriorhodopsin and its relation to protein stability. *Biophysical Journal*, **94**:3647–3658.

Shen, W., Ji, S., Chen, L., Zhang, Y., & Wu, X. (2018) Synthesis and properties of alkoxyethyl β-D-xylopyranoside. *Journal of Surfactants and Detergents*, **21**:255–267.

Smułek, W., Kaczorek, E., & Hricovíniová, Z. (2017) Alkyl xylosides: Physico-chemical properties and influence on environmental bacteria cells. *Journal of Surfactants and Detergents*, **20**:1269–1279.

Vill, V., Böcker, T., Thiem, J., & Fischer, F. (1989) Studies on liquid-crystalline glycosides (1989). *Liquid Crystals*, **6**:349–356.

von Minden, H. M., Brandenburg, K., Seydel, U., Koch, M. H. J., Garamus, V., Willumeit, R., & Vill, V. (2000) Thermotropic and lyotropic properties of long chain alkyl glycopyranosides. Part II. Disaccharide headgroups. *Chemistry and Physics of Lipids*, **106**: 157–179.

Wang, F., & Zhang, Y.-Q. (2017) Effects of alkyl polyglycoside (APG) on *Bombyx mori* silk degumming and the mechanical properties of silk fibroin fibre. *Materials Science & Engineering C-Materials for Biological Applications*, **74**:152–158.

Weber, N., & Benning, H. (1984) Metabolism of orally administered alkyl β-glycosides in the mouse.*Journal of Nutrition*, **114**:247–254.

Whorton, M. R., & MacKinnon, R. (2013) X-ray structure of the mammalian GIRK2–βγ G-protein complex. *Nature*, **498**:190–197.

Wu, H., Bao, Y., Wang, X., Zhou, D., & Wu, W. (2017) Alkyl polyglycoside, a highly promising adjuvant in intranasal split influenza vaccines. *Human Vaccines & Immunotherapeutics*, **13**:1279–1287.

Xiao, J., Zhao, L., & Shen, Z. (2017) Enhanced sludge anaerobic fermentation using microwave pretreatment combined with biosurfactant alkyl polyglycoside. *RSC Advances*, **7**:43772–43779.

Yelamaggad, C. V., Mathews, M., Hiremath, U. S., Rao, D. S. S., & Prasad, S. K. (2005) Self-assembly of chiral mesoionic heterocycles into smectic phases: A new class of polar liquid crystal. *Tetrahedron Letters*, **46**:2623–2626.

Zhang, L., Somasundaran, P., & Maltesh, C. (1996) Electrolyte effects on the surface tension and micellization of n-dodecyl β-D-maltoside solutions. *Langmuir*, **12**:2371–2373.

Zhao, H., Bai, Y., Sun, H., & Li, Y. (2017) Study of the molecular array behaviours and interfacial activities of green surfactant alkyl polyglycoside and the mixed systems with other surfactants on oil–water interface. *Molecular Simulation*, **43**:1107–1115.

Zheng, W., Shen, Y., & Lu, W. (2007) Determination of high purity soybean lecithin HLB by NMR.*Cereals & Oils*, **7**:39–41 (in Chinese).

Zhou, J., & Cui, Y. (2001) Measurement and calculation of HLB value of surfactants I. The measurement of HLB value. *Speciality Petrochemicals*, **2**:11–14 (in Chinese).

Zhou, J., Cui, Y., & Wu, Y. (2001) Measurement and calculation of HLB value of surfactants II. The calculation of HLB value. *Speciality Petrochemicals*, **4**:38–41 (in Chinese).

Zhou, Y., Wang, S., Lv, M., Niu, J., & Xu, B. (2017) Analysis of the effects of hydrocarbon chain on foam properties of alkyl polyglycosides.*Journal of Surfactants and Detergents*, **20**:623–630.

Biographies

Zhencao Li is currently a researcher in STA Pharmaceutical Co., Ltd. He obtained his B.Sc. in pharmacy from Jining Medical University in 2013, his M.Sci. in Chemistry from Xiangtan University. His research interests focus on sugar-based surfactants, organic synthesis, and pharmaceutical synthesis.

Guoyong Chen is currently a researcher in STA Pharmaceutical Co., Ltd. He obtained his B.Eng. in polymer materials and engineering from Ludong University in 2013, his M.Eng. in chemical engineering from Xiangtan University. His research interests focus on pharmaceutical synthesis and sugar-based surfactants.

Prof. (Dr.) Langqiu Chen is currently a professor in the College of Chemistry at Xiangtan University. He received his B.Sc. in chemistry from Xiangtan University (China) in 1984, his M.Eng. in food Engineering from Light Industry Institute of Tianjin (China) in 1990, and his Ph.D. from the Graduate School of Chinese Academy of Sciences (Research Center for Eco-Environmental Science, Academia Sinica) (China) in 2003, respectively. He worked as a guest researcher in Ryukoku University (Japan), supported by JSPS for 10 months and as a postdoctoral researcher in the Department of Chemistry at the University of Oxford (United Kingdom) for 1 year. His research interests focus on carbohydrate chemistry, sugar-based surfactants, organic synthesis, pharmaceutical synthesis, and food additives.

Yanhua Zhang has just received her M. Sc. from College of Chemistry, Xiangtan University. She obtained her B.Sc. in chemistry from Hengyang Normal University (China) in 2015. Her research interest includes the synthesis and aggregation behaviors of sugar-based surfactants.

Zhiyong Dai is currently a researcher in Ausnutria Dairy (China) Co. Ltd. He obtained his B.Sc. in Chemistry from Xiangtan University in 1997, his M.Ag. in food processing from Central South University of Forestry and Technology in 2017. His research interests focus on sugar, Protein, Animal milk, and food processing technology.